Designed a Spectrophotometric Method for the Determination of Tartrazine Residual in Different Drinks and Foodstuffs by Using *Mandarin leaves*-Capped Gold Nanoparticles

Marahel, Farzaneh[*+]

Department of Chemistry, Omidiyeh Branch, Islamic Azad University, Omidiyeh, I.R. IRAN

ABSTRACT: *Tartrazine color is a synthetic organic food dye that can be found in common food products such as bakery products, dairy products, candies, and beverages, the presence and content of tartrazine color must be controlled in food products due to their potential harmfulness to human beings. Although the liquid chromatographic, and other methods for tartrazine color have advantages such as excellent accuracy and reproducibility, it has limitations such as long-time measurement, and high equipment costs. In this study, to determine tartrazine color in the solution we used a prepared from Mandarin Leaves-capped AuNPs sensor and kinetic spectrophotometric method. The calibration curve was linear in the range of (0.02 to 12.0 µg/L). The standard deviation of (3.0%), and detection limit of the method (0.02 µg/L in time 7 min, 385 nm) were obtained for sensor level response Mandarin Leaves-capped AuNPs with (95%) confidence evaluated. The observed outcomes confirmed the very low detection limit for measuring the tartrazine color in food samples. The artificial neural network model was used as a tool very low for determining mean square error (MSE = 0.515) for tartrazine color by Mandarin Leaves-capped AuNPs sensor. The chemical Mandarin Leaves-capped AuNPs sensor made it possible as an excellent sensor with reproducibility.*

KEYWORDS: *Tartrazine color (TZ); Foodstuff; Neural network model; Kinetic spectrophotometric; Sensor.*

INTRODUCTION

Food dyes are often added to foodstuffs and drinks in order to supply, tartrazine (TZ) color is a synthetic organic food dye that can be found in common food products such as bakery products, dairy products, candies, and beverages. Due to the toxic nature of some dyes, mutagenic impacts of them, and skin disorders (irritation and allergies) related to them, the potential pollution of dyes and their intermediates has drawn the attention of many researchers [1]. In addition, microbial degradation of synthetic dyes due to carcinogenic impact of benzidine and other aromatic compounds has been a matter of health concern [2,3]. The presence and content of TZ dye must be controlled in food products due to their potential harmfulness to human beings [4]. Therefore, the determination of tartrazine (TZ) color in commercial food products is very important. Until now, different methods such as Chromatography [5]. Chromatographic by HPLC [6], Colorimetry [7], Oxidation [8], flow injection [9], adsorption [10], and spectrophotometry [11,12], have been

reported among the most used methods in determining TZ color. Regardless of how time-consuming these techniques are yet, they need advanced instrumentation and are not fit for real-time analysis. Accordingly, developing a simple, quick, elective, and delicate method like spectrophotometric measurement in determining

Tartrazine (TZ) color was highlighted. In this method, sensing tartrazine (TZ) color was done with high sensitivity and excellent selectivity for discerning and accurate reorganization of species (1-inorganic 2- organic and 3- biomolecules) in different intricate matrices, attention has been drawn to noble metal nanoparticles-based UV–Visible spectrometric methods [13,14].

In the last decade, some chemical sensors have been developed using several kinds of materials to improve selectivity, and stability and has been material included various nano-materials such as metal NanoParticles (NPs), metal oxide NPs, polymeric NPs, carbon-based nanomaterials and quantum dots [15,16]. A wide variety of nanocomposites have been recently applied to fabricate the modified sensors because of their biological compatibility, high-specific surface area, chemical stability, excellent catalytic activity and conductivity [17]. Among these catalysts, carbon-supported transition-metals (M-N-C, M = Co, Fe, Ni, Mn, etc.) have attracted considerable attention owing to their low-cost and high catalytic activity poisoning resistances [18].

Due to the profitable application of metal nanoparticles, technologies have taken advantage of nanoscale materials in a variety of fields from chemistry to medicine. To improve the selective interaction between analyses and the sensing layer, chemically modified matrices have been used. The applied matrix has enhanced the conductivity, surface area, and sensitivity [19,20]. The production of nanoparticles using the principles of green chemistry has found a special place in research and for this purpose, various types of biological systems are used. The use of microorganisms, diatoms, and optical eukaryotes are among these systems, but due to the high costs for their preparation and maintenance are less used. Today, plants and agricultural products have received special attention as renewable and cheap sources for the production of biological nanomaterials [21,22].

Recovery of nanoparticles from plant tissue is tedious, expensive and requires enzymes to destroy plant cellulose tissue. Therefore, it is easier to use plant extracts in low processing and large scale to prepare various metal nanoparticles. In recent years, the use of plant extracts for the preparation of metal nanoparticles has been proposed as an easy and suitable alternative to chemical and physical methods [23]. The forms, sizes, and structures of metallic nanomaterials which are extensively linked to their chemical, physical, and optical characteristics, set the ground for successful using them in technologies. In this respect, the exceptional physical, chemical, and biological properties of AuNPs has been widely used. This exceptionality arises from the size, form, composition, crystallinity, and structure of AuNPs in comparison with its bulk form [24]. AuNPs can be by various methods such as the application of stabilizing and reducing chemicals of hydrate and sodium borohydride, chemical heating, and photochemical reduction prepared [25]. The *Mandarin* tree grows in many regions indicating that this biosensor derived from *Mandarin* is very inexpensive, energy-saving, and most important of all non-toxic. Fast and clean synthesis without the use of toxic and dangerous compounds or surfactants as a highly stable and reusable eco-friendly catalyst under solvent-free conditions and excellent yield in a short time. Also, the use of sodium borohydride extract as an economic and effective reducing and stabilizing agent these characteristics makes *Mandarin Leaves*-capped AuNPs sensor a potential biosensor for tartrazine color measurement when juxtaposed against other commercial materials [26]. Herein, *Mandarin Leaves*-capped AuNPs with were first synthesized successfully and utilized for the fabrication of sensitive and specific sensors toward TZ color activity with the help $NaBH_4$ as an economic and effective reducing and stabilizing determining for TZ color by sensors operate based on the induced color change from the aggregation of Au nanoparticles after the formation of the complex. As shown in (Scheme. 1), AuNPs nanoparticles led to the formation of *Mandarin Leaves*-capped AuNPs-TZ color assembly in the presence of sodium borohydride. The sensitivity of the *Mandarin Leaves*-capped AuNPs platform was significantly enhanced owing to the high absorbing efficiency of Mandarin Leaves to TZ color. Meanwhile, with the combination of the high affinity of TZ color with Au as well as the huge specific area of the Mandarin Leaves scaffold, the fabricated *Mandarin Leaves*-capped AuNPs can reversibly enrich ~95.0% of TZ color in water samples [16, 19, 27].

This study, was to evaluate the use of an Artificial Neural Network (ANN) model to predict the determination TZ
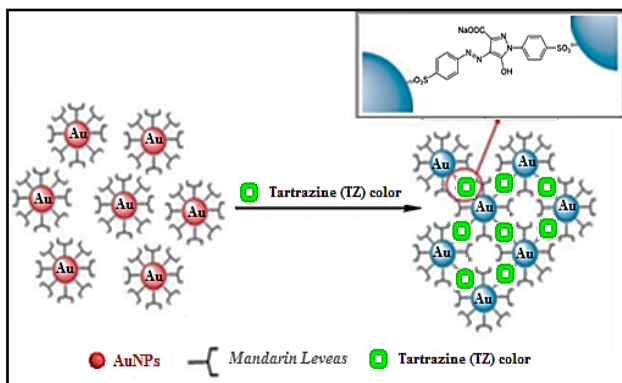
Scheme 1: Schematic Illustration of the reaction between TZ color and Mandarin Leaves based AuNPs.

color in solution by *Mandarin Leaves*-capped AuNPs. ANN is a numerical estimation technique, which is used to find nonlinear relationships between input and output variables. In this research, for measure TZ color various effective factors such as (pH, tartrazine color concentration, *Mandarin Leaves*-capped AuNPs concentration, time Reaction, etc.) on the response of the method and obtaining the optimal test values and obtaining the linear range, detection and accuracy of the method presented in the measurement of TZ color by a kinetic Spectrophotometric new method in real samples was checked. The chemical *Mandarin Leaves*-capped AuNPs sensor made it possible as an excellent sensor with reproducibility, good recovery and a very low detection limit for measuring TZ color. The method by kinetic Spectrophotometric was introduced to measure tartrazine (TZ) color in food samples and can be used for other samples.

EXPERIMENTAL SECTION
Reagents and materials

All chemicals including (HAUCl$_4$) and Sodium borohydride (NaBH$_4$) were provided by Merck Company while TZ color (98.0%) was purchased from India Company. For pH < 7.0, buffer solutions were prepared from 1 mL of boric acid/acetic acid/phosphoric acid (1.0 M), and for pH >7.0 was adjusted by the addition of 0.2M sodium hydroxide, DD H$_2$O (Double distilled water) was used in the preparation of the solutions.

Instrumentation

UV–Vis spectrophotometer (Model UV–Vis Shimadzu 180, Japan). The registration of FT-IR or Fourier transform infrared spectra was done on a PerkinElmer (FT-IR

spectrum BX, Germany). SEM (Scanning electron microscopy: KYKY-EM 3200, Hitachi Firm, China) under an acceleration voltage of 26kV) was used to study the morphology of samples. Transmission electron microscopy (TEM) images were taken on a (JEOL 3010, Hitachi Company, China). X-ray diffractometer (D5005, Siemens, Germany), with Cu-Kα, operating voltage 50 kV, operating current (tube current) 150 mA.

Pretreatment of real samples

In a 50 mL beaker, treatment of a 10 mL portion of strawberry jelly (Tehran, Iran), fruity candy (Ben Ben, Iran), Smarties (Morvarid, Iran), gummy candies (YupiIndonesia), Noshmak (Tehran, Iran) and jell gum with fruit taste (Shiba Co) (PASTIL) samples were dissolved in warm water, filtered if necessary, (or a spiked samples) and diluted in a volumetric flask. An aliquot of the above sample solutions was treated under the general procedure for ATPS and subsequent determination of TZ color [28].

Synthesis of Mandarin Leaves-capped AuNPs

In this regard, the following details of the materials are important to consider in their synthesis: surface property, size distribution, apparent morphology, particle composition, and dissolution *Mandarin Leaves*-capped AuNPs were Prepared by the Reduction of HAUCl$_4$ with NaBH$_4$ as a modifier according to the method in the literature [29]. Briefly, 10.0 mL *Mandarin Leaves* (2.0 mM) the solution was added into the reaction flask that contained 1.0 mL of HAUCl$_4$ (2.0 mM) under vigorous stirring. After 15 min, 1.0 mL of NaBH$_4$ (2.0 mM) was added to the above solution at room temperature and stirred for 1 h. UV–Visible spectrum of *Mandarin Leaves*-capped AuNPs. The inset picture shows *Mandarin Leaves*-capped AuNPs. The dark colloidal solution color was changed to bright yellow, confirming the formation of *Mandarin Leaves*-capped AuNPs. The *Mandarin Leaves*-capped AuNPs solution was stored in the dark at $4.0 \pm 2.0 °$C to remain stable for several weeks (Fig. 1).

Artificial neural network

In recent years in different fields of science, various applications of artificial neural network models were provided. Therefore, the application of intelligent systems, including the use of artificial neural networks, is expanding
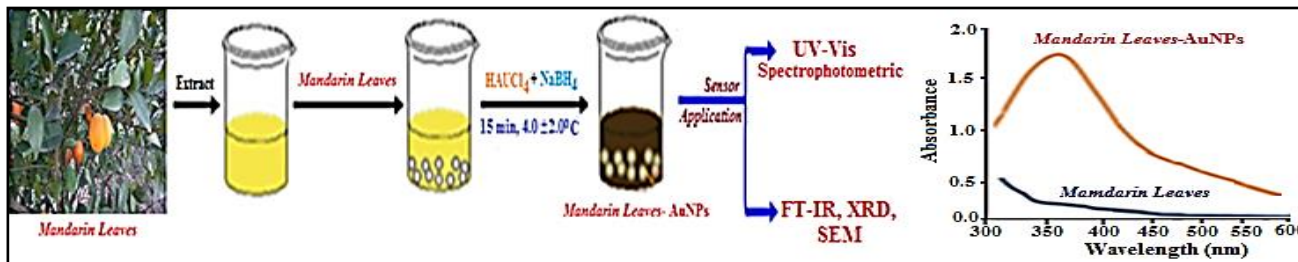
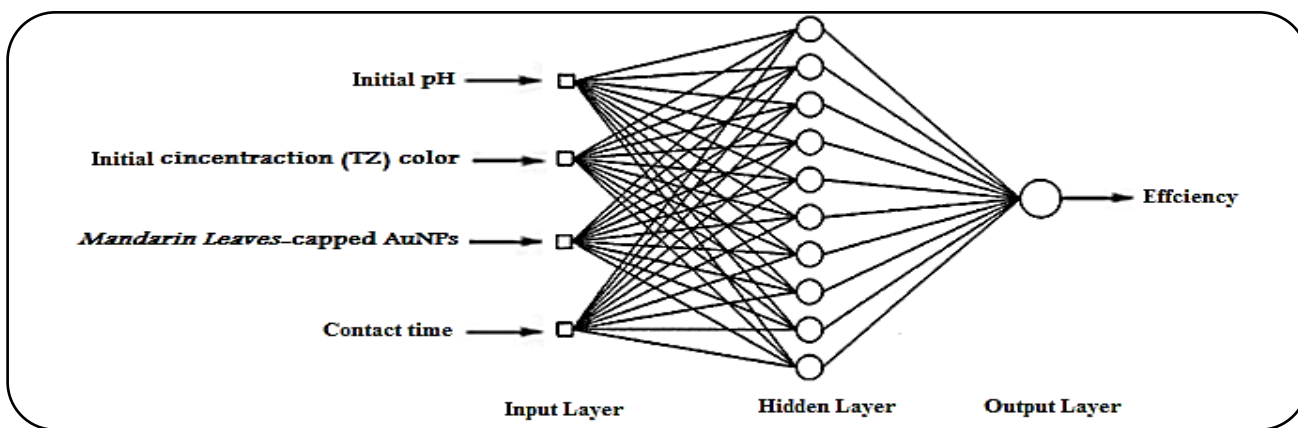*Fig. 1: Synthesis of Mandarin Leaves-capped AuNPs.*

Fig. 2: Architecture of neural network system.

to model complex systems. The artificial neural network can accurately describe complex and nonlinear relationships with precise rules. These systems play an important role in optimizing food formulation, developing quality measurement tools, and modeling food processes. Due to the high accuracy artificial neural network is one of the best tools to predict the results of processes using laboratory data. Similar studies confirm this fact. In this research, modeling was done by MATLAB software. To identify this model, also we must introduce our data to software in normalized view [30].

In the network, neurons are organized in several layers. These layers are: the input layer, a hidden layer or layers (middle) and (MLP) layer of perceptron which are multilayer output. Each neuron is connected to all neurons in the next layer, but there are no connections between neurons in a layer. In Artificial Neural Network (ANN), feed-forward back propagation was employed as the training algorithm. The final computed data for FFBP were juxtaposed against the experimentally attained findings. A model ANN with four input layers (initial TZ color concentration, Au/*Mandarin Leaves* dosage, pH, and time) was detected at epoch numbers 10, and 22 experimental points were employed to feed the model (Fig.2). The MSE

based on the function of error performance showed a minimum value at 5 neurons, from training, test, and data points, respectively, and the data set was derived. In the present study, the Levenberg-Marquardt backpropagation algorithm was used for the network [31].

This algorithm: All samples were normalized between 0-1, to achieve fast convergence, commensurability of the scale of the input, as well as the minimal R_{MSE} values. The normalized values of data were obtained according to Eq. (1):

$$X_{norm} = \frac{X - X_{min}}{X_{max} - X_{min}} \tag{1}$$

Where X is a variable, but X_{min} and X_{max} refer to the minimum value and the maximum value, respectively. Statistical parameters: correlation coefficient (R^2), the Mean Squared Error (MSE), Total Squared Error (SSE), The Relative Mean Error (AARE), And Standard Deviation (SD) are calculated through Equations (2-6), respectively [31,32].

$$R^2 = \frac{\sum\left(Y_{exp,i}-Y_{model,mean}\right)^2 - \sum\left(Y_{model.i}-Y_{exp,i}\right)^2}{\sum\left(Y_{exp,i}-Y_{model,mean}\right)^2} \tag{2}$$

$$MSE = \frac{\sum(Y_{model.i} - Y_{exp,i})^2}{n} \tag{3}$$

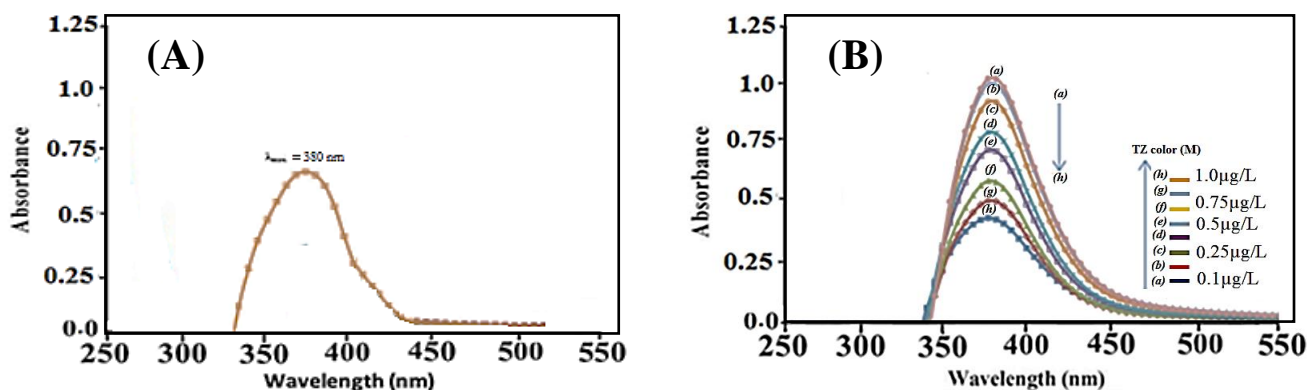$$SSE = \sum(Y_{model.i} - Y_{exp,i})^2 \tag{4}$$

Fig. 3: A) The absorption of TZ color B) The absorption of result Mandarin Leaves-capped AuNPs and TZ color 30 sec, and increasing concentration of TZ color solution (0.25 µg/L).

$$AARE = \frac{1}{n}\Sigma\left(\left|\frac{Y_{exp,i} - Y_{model.i}}{Y_{exp,i}}\right|\right) \qquad (5)$$

$$SD = \sqrt{\frac{1}{n-1}\Sigma\left(\left|\frac{Y_{exp,i} - Y_{model.i}}{Y_{exp,i}}\right| - AARE\right)^2} \qquad (6)$$

Procedure kinetic Spectrophotometric Detection measurements

The ensuing steps have been considered for a kinetic Spectrophotometric method experiment in the current study, at the initial step: Some of the sample solution containing 1mL of TZ color (10.0 µg/L) was added to a 10 mL volumetric balloon. Then 1 mL of utilizing sodium borohydride as a stabilizer for sensor (2.0×10^{-2} mol/L) was added to the flask. Now, by increasing the first drop of 1 mL of *Mandarin Leaves*-capped AuNPs solution (2.0×10^{-2} mol/L) into a balloon, the reaction start time is recorded by a timer, after 5 seconds from the start of the reaction the solution is stirred for 30 seconds, Subsequently, an adequate amount of the solution was added to a 1 cm cell. Finally through using of UV–Visible spectrum (AAb), the measurement of the difference between the quantities of the absorption in wavelength equal to (385.0 nm) in a time interval (1.0 -7.0 min) was carried out.

By adding TZ color to the solution, it was observed that absorbance kinetic Spectrophotometric of the *Mandarin Leaves*-capped AuNPs at the wavelength of (385 nm) dropped, this is because TZ color in the wavelength of (380 nm) forms a complex with some intermediate metals in sensors and transmits the absorption peak to shorter wavelengths at the wavelength of (385 nm). At the same time, with the help of spectrophotometry and UV–Visible spectrum (AAb), the apparent spectral evolution including

the formation of a well-defined isobestic point at around (385.0 nm) was estimated. All reaction steps were repeated by increasing the concentration (0.25 µg/L) of the TZ color every 30 seconds. Moreover, the mentioned steps were repeated for a reaction in the absence of TZ color (Abs b). Eventually, (Abs a) Abs blank – Abs sample was calculated. The reaction of the TZ color by *Mandarin Leaves*-capped AuNPs was detected in the acidic medium in its wavelength (385 nm). Fig. 3A and 3B, demonstrate the absorption spectra in an aqueous solution [8, 33].

RESULTS AND DISCUSSION
Characterization of sorbent

In Fig. 4a, the FT-IR spectrum of activated carbon prepared from *Mandarin Leaves*-capped AuNPs is shown. Additionally, the observed absorption signal at 3391 cm^{-1} points to O-H groups' presence because of the alcoholic or phenolic functional groups. Also, the presence of C-H groups is well proven by the signal observed at 2930 cm^{-1}. Correspondingly, the C=C active group's presence is confirmed by the signal observed 1425.7 at 1642 cm^{-1}, the C-O active group's presence is confirmed by the signal observed at 1035.4 cm^{-1}. The signal at 776.8 cm^{-1} is relevant to the Au-O group of the *Mandarin Leaves*-capped AuNPs [34]. Different X-ray emission peaks are *Mandarin Leaves*-capped AuNPs shown in (Fig. 4b). The signals at 38.5 (122), 45.0 (111), 52.2 (200), 54.4 (231), and 72.7 (220) are ascribable to diffractions and reflections from the carbon atoms [35]. The perfect crystalline nature of the material was proven after functionalizing with *Mandarin Leaves*-capped AuNPs however the great intensity of the signal at 45.0 (111) confirmed that there has been a slight amount of material in an amorphous state.
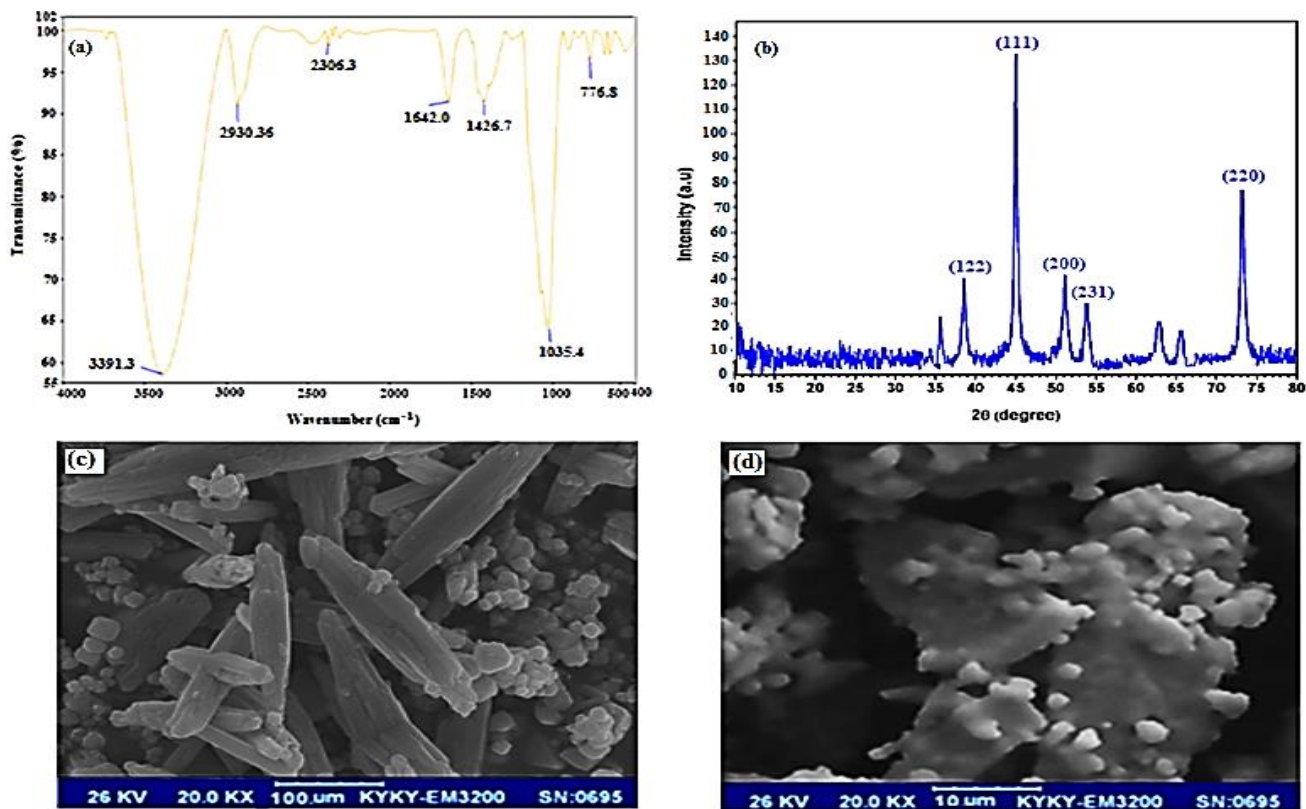
Fig. 4: (a) FTIR spectra of the prepared Mandarin Leaves-capped AuNPs. (b) Different X-ray emission peaks are Mandarin Leaves-capped AuNPs. (c) The (SEM) image of the prepared Mandarin Leaves-capped AuNPs in 100 nm (d) The (SEM) image of the prepared Mandarin Leaves-capped AuNPs in 10 nm.

The morphological properties of the samples scrutinized by SEM are exhibited. By looking at (Fig. 4c and 4d). After surface modification, the *Mandarin Leaves*-capped AuNPs became uneven, larger, and bundled [36].

Optimization of decomposition

It would be interesting to know that in the presence of TZ color, there observed a considerable improvement in the effectual colorimetric sensing and absorbance kinetic Spectrophotometric method of the as-prepared *Mandarin Leaves*-capped AuNPs. Obtaining an exceptionally sensitive response in detecting TZ color rests upon the systematic optimization of pH values, *Mandarin Leaves*-capped AuNPs, and incubation time.

In this section, the best type of buffer and its volume for maximum absorption TZ color with *Mandarin Leaves*-capped AuNPs sensor are investigated. To this step, the procedure is as follows: In 10 mL balloons, separately 1 mL of TZ color (10.0 µg/L) and a volume of each type of acetic acid / boric acid / phosphoric acid buffer and then 1mL of 1 *Mandarin Leaves*-capped AuNPs (2.0×10^{-2} mol/L),
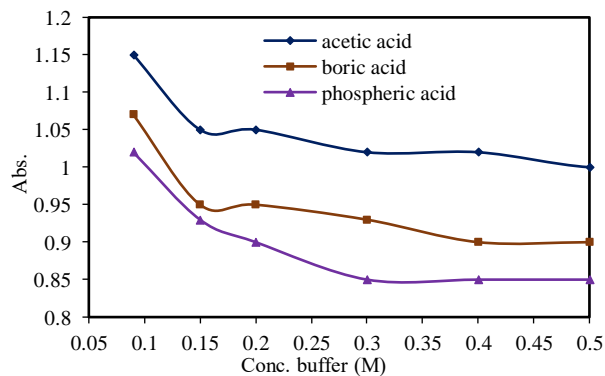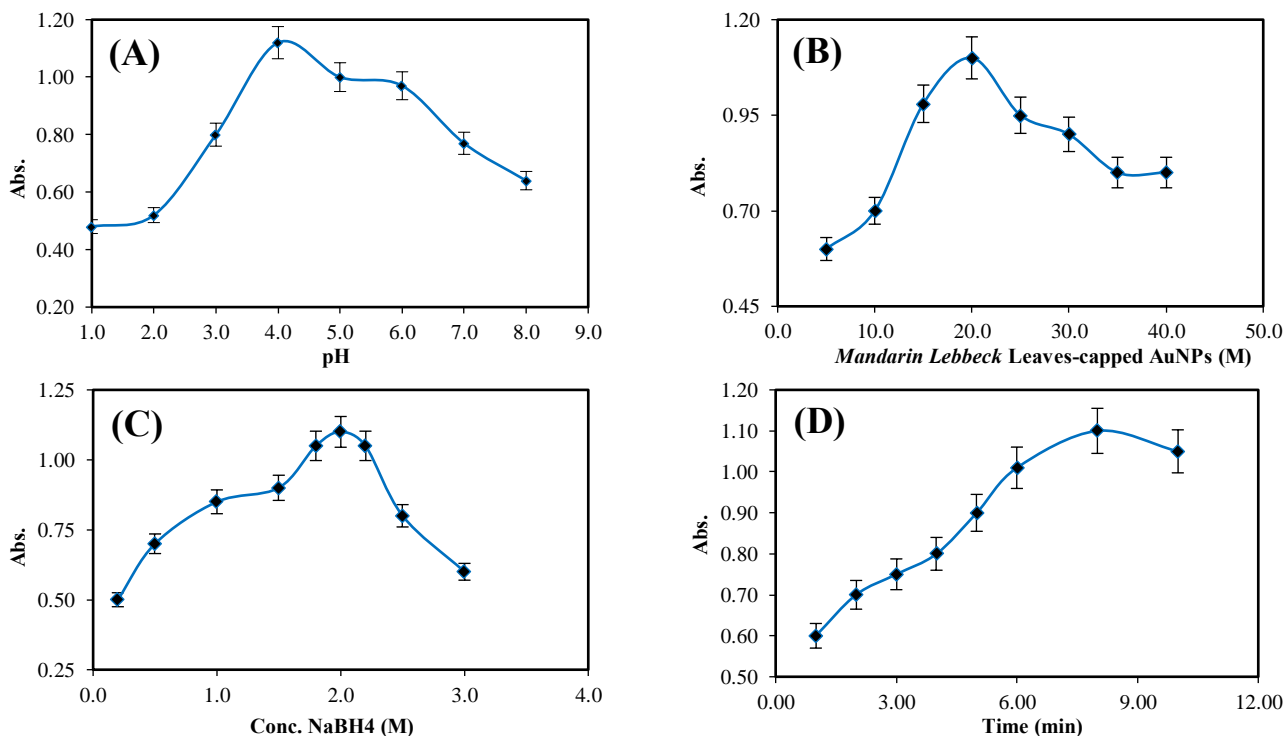

Fig. 5: The impact of buffer concentration on the absorbance, aqueous sample volume, 10 mL in385 nm. (Mandarin Leaves-capped AuNPs, 2.0×10^{-2} M, sodium borohydride, 2.0×10^{-3} M, TZ color = 10.0 µg/L, time 7 min).

1mL utilizing sodium borohydride as a stabilizer for sensor (2.0×10^{-3} mol/L), to the solution inside the balloon and after (7 minutes), the adsorption of the solution was read by UV–Visible spectrophotometry. The results are shown in (Fig. 5). Based on the results, 1 mL of acetic acid buffer shows the highest percentage for the determination of TZ

Fig. 6: (A) The impact of pH on the absorbance, aqueous sample volume, 10 mL in 385 nm. (Mandarin Leaves-capped AuNPs, 2.0×10^{-2} M, sodium borohydride, 2.0×10^{-3} M, TZ color = 10.0 µg/L, time 7 min). (B) The impact of starch-capped AgNPs on the absorbance. (Sodium borohydride, 2.0×10^{-3} M, pH =4, TZ color = 10.0 µg/L, time 7 min). (C) The impact of sodium borohydride on the absorbance. (Mandarin Leaves-capped AuNPs, 2.0×10^{-2} M, pH =6, TZ color =10.0 µg/L, time 7 min). (D) The impact of time on the absorbance. (Mandarin Leaves-capped AuNPs, 2.0×10^{-2} M, sodium borohydride, 2.0×10^{-3} M, pH =4, TZ color = 10.0 µg/L).

color, so acetic acid /tri chloric acetate buffer (1.0 M) to adjust the pH solution as the optimal buffer.

The great impact of the pH value of the reaction solution on the interaction between *Mandarin Leaves*-capped AuNPs and TZ color was undeniable. To examine the influence of *Mandarin Leaves*-capped AuNPs on the reaction rate, 1mL TZ color (10.0 µg/L) solution, *Mandarin Leaves*-capped AuNPs (2.0×10^{-2} mol/L), and 1 mL sodium borohydride (2.0×10^{-3} mol/L) were mixed in the 10 mL volumetric flask using DD H_2O (Double distilled water).

After measuring the absorbance intensity of the solution, a thorough investigation was carried out on the absorbance pH values in the range of (1-8) for the TZ color- *Mandarin Leaves*-capped AuNPs complex at (385 nm). As evident in (Fig. 6A), absorbance kinetic Spectrophotometric rapidly on changing the pH from 1.0 to 4.0, while it decreased at pH values higher than 4.0. This phenomenon might be because of the weak complexion at lower pH values (pH <4.0). On the other hand, the reduced response of the proposed *Mandarin Leaves*-capped AuNPs sensor for determining TZ color at pH > 4.0 could be due to a possible formation of the

hydroxide of TZ color in solution. Thus, pH 4.0 was selected as a favorable pH for all subsequent experiments. Concurrently, 1 mL TZ color (10.0 µg/L) solution, 1 mL sodium borohydride (2.0×10^{-3} mol/L) and 1mL *Mandarin Leaves*-capped AuNPs (0.5×10^{-3} to 4.0×10^{-2} mol/L), were mixed in a volumetric flask 10 mL using DD H_2O (Double distilled water) to find out about the impact of *Mandarin Leaves*-capped AuNPs on the reaction rate. Again the absorbance intensity of the solution was assessed. The previously mentioned operation has been replicated for blank solution (the solution in the absence of TZ color). The findings are exhibited in (Fig. 6B). Consequently (2.0×10^{-2} mol/L) based on those findings was determined as the perfect concentration [23, 37].

To look over the efficacy of sodium borohydride concentration, with a help of volumetric flask 10 mL firstly 1 mL TZ color (10.0 µg/L) solution, 1 mL sodium borohydride with different concentration (0.05 to 3.0×10^{-3} mol/L), and 1 mL *Mandarin Leaves*-capped AuNPs, (2.0×10^{-2} mol/L) Again after (7.0 min) sharp, the estimation for sorption of solution was carried out.

Table 1: Investigation of method repeatability at conditions.

| Parameter	Optimum Value for tartrazine (TZ) color
TZ color (M)	(10.0 µg/L)
Mandarin Leaves-capped AuNPs (M)	$(2.0 \times 10^{-2} \text{ M})$
concentration $NaBH_4$ (M)	$(2.0 \times 10^{-3} \text{ M})$
pH	4.0
Equilibration time (min)	(7.0 min)
Linear range (LDR)	(0.02 - 12.0 µg/L)
Detection limit (LOD)	(0.02 µg/L)
Relative Standard Deviations (RSD)	(1.9 %)
Accuracy and precision	High
Advantages	High repeatability, sensitivity, selectivity, accuracy, precision, wide linear range, and no need to use organic solvents
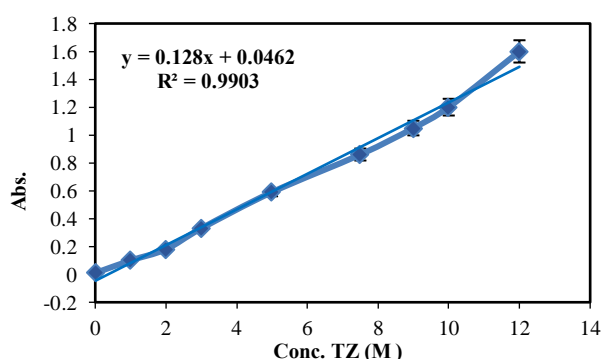
Fig. 7: Calibration graph for TZ color, aqueous sample volume, 10 mL in 385 nm. (Mandarin Leaves-capped AuNPs 2.0×10^{-2} M, sodium borohydride, 2.0×10^{-3} M).

The aforementioned steps were repeated in the absence of TZ color (blank solution). The findings are exhibited in (Fig. 6 C). The decision on the desired concentration for sodium borohydride based on the results was made to be $(2.0 \times 10^{-3} \text{ mol/L})$. Also, the impact of reaction time on the absorbance spectrum was investigated. Based on (Fig. 6D), it has become apparent that the absorbance intensity enhanced expeditiously and reached its peak at around 7 min. After 7 min, relative stability was spotted in the absorbance intensity. Thus, 7 min was determined as the perfect reaction time in this experiment [38, 39].

Measurement of Tartrazine (TZ) color in standard solutions and calibration

Analytical performance of *Mandarin Leaves*-capped AuNPs sensor for determination of TZ color. Under the optimum condition, were recorded for different concentrations of TZ color onto the *Mandarin Leaves*-capped AuNPs.

The absorbance kinetic Spectrophotometric peaks with two linear range of (0.02–12.0 µg/L) for TZ color were obtained respectively. The linear regression equation and R^2 of TZ color were

$y = 0.128C_{TZ} + 0.0462$ and 0.9903, respectively (Fig. 7). Also, for 7 replicates measurement of TZ color (10 µg/L), the solution with optimized conditions, the relative standard deviation (R.S.D) for the response of *Mandarin Leaves*-capped AuNPs towards a (10 µg/L) of TZ color was (1.9 %) and reproducibility of the response of different *Mandarin Leaves*-capped AuNPs was also studied. The determination of (10.0 µg/L) TZ color. The relative standard deviation for the response of *Mandarin Leaves*-capped AuNPs was (0.02 µg/L) [13,40].

Optimum values of parameters

The optimum values of parameters are demonstrated in Table.1. The method can be used as an alternative method for TZ color measurement owing to advantages like excellent selectivity and sensitivity, low cost, simplicity, low detection limit and no need in utilizing organic harmful solvent.

Modeling of artificial neural network process

The three functions of weight (training), net input, and transfer (tansig) governed the performance of the network. A mean square error (MSE=0.515) was detected at epoch numbers 10 and 22 experimental points were employed to feed the model for determining of TZ color. In the (Fig. 8 to Fig. 10), the plots of errors histogram for the adsorption processes are demonstrated indicating that the errors in this removal processes are low. During the net training

Table 2. Statistical comparison of models of artificial neural network.

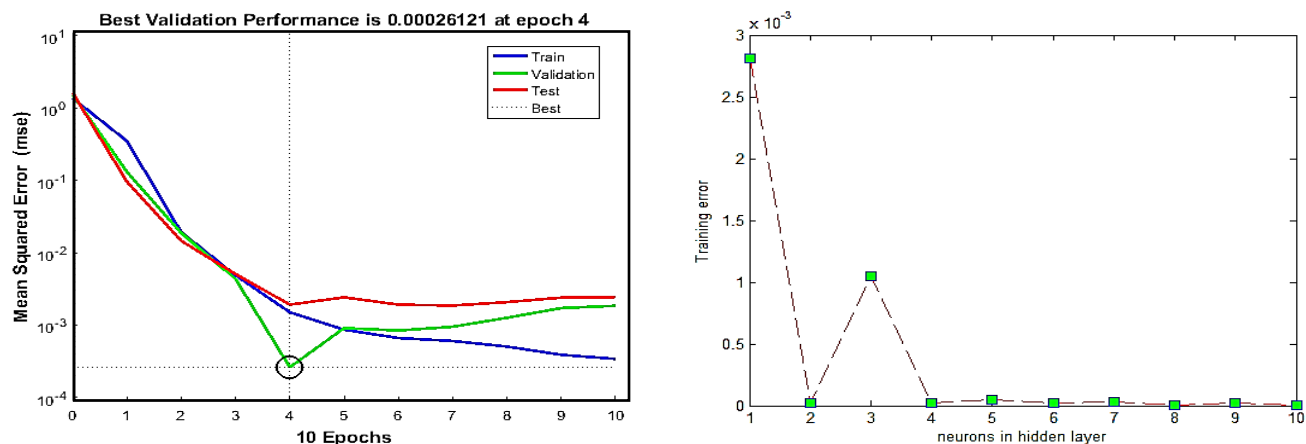| Modeling	SSE	MSE	AARE	SD	R^2
ANN	10.815	0.515	0.0314	0.4539	0.9999

Fig. 8: Evolution of training, validation, and test errors as a function of the number of training epochs during ANN for the TZ color determining by Mandarin Leaves-capped AuNPs sensor.
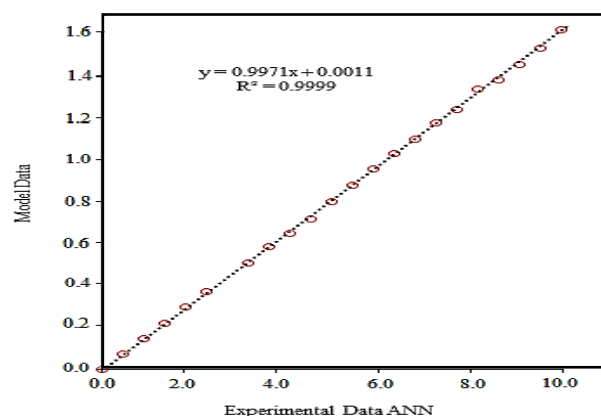

Fig. 9: Neural Network Outputs in Test and Total Data Stages for determining the TZ color determined by Mandarin Leaves-capped AuNPs sensor synthesis percentage is demonstrated Process.
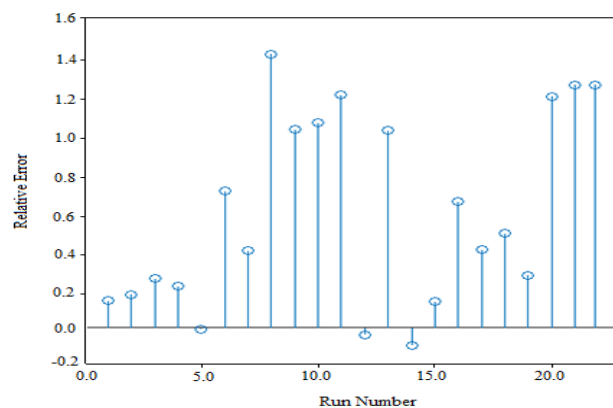

Fig. 10: The plot of Relative error histogram for determining on the TZ color determining by Mandarin Leaves-capped AuNPs sensor synthesis percentage is demonstrated Process.

process in this study, the MSE based on the function of error performance showed a minimum value at 5 neurons [31, 32]. A model ANN with four input layers (viz., initial TZ color concentration, *Mandarin Leaves*-capped AuNPs dosage sensor, pH, and time) based on the output layers (determining of target compounds) as shown in (Table. 2), Statistical parameters R^2, MSE, SSE, AARE and SD are calculated found to be adequately accurate for predicting and estimating the TZ color in samples respectively [32].

The summary results relative of parameters the model are compared in Table. 2. The lowest determination error TZ color by *Mandarin Leaves*-capped AuNPs sensor in demonstrated Process.

Interference studies

After establishing the measurement method, to evaluate the selectivity of the prepared *Mandarin Leaves*-capped AuNPs sensor for determining the TZ color the effect of various substances on the determination of TZ (10.0 µg/L) for method respectively was tested under optimum conditions. Several representative potential interferences such as inorganic cations, anions, molecular species and dyes were investigated individually for their effect on TZ recovery. As exhibited in (Table. 1), the tolerance limit was determined as the max concentration of the interfering substance which resulted in an error less than (±5%) for measure of TZ in real samples [11,40].

Table 3. Impacts different foreign species on the retrieving of TZ color (n=3).

Foreign species	Tolerance limit (µg/L)
Glucose, Lactose, Sunset yellow, Folic Acid, Allure red	1000
Oxalate, Tartrate, Citrate, Malic acid	750
NH_4^+, Mg^{2+}, Ca^{2+}, Ag^+, Cu^{2+}, Fe^{3+}, Cl^-, F^-, I^-	500
Ascorbic Acid, Vitamin A, Vitamin D	350
Vitamin B1, Vitamin B12, Vitamin B6	250

Table 4. Determination of TZ color in spick color drink and foodstuff samples (n=3).

Samples	Spiked concentration of TZ (µg/mL)	Proposed method TZ (µg/mL)	t_{exp}	Recovery %
Jell Gum	0.00	0.74 ± 1.1	0.96	----
	0.50	1.25 ± 1.2		104.0
Fruity candies	0.00	0.42 ± 1.1	1.13	----
	0.50	0.93 ± 1.4		102.0
Jelly stra wberry	0.00	0.28 ± 1.7	0.95	----
	0.50	0.79 ± 1.8		101.9
Gummy candies	0.00	1.49 ± 3.8	2.31	----
	0.50	1.96 ± 3.0		94.0
Noshmak	0.00	0.44 ± 2.3	1.42	----
	0.50	0.95 ± 1.8		102.0
Smarties	0.00	0.66 ± 1.5	1.39	----
	0.50	1.15 ± 1.1		98.0

Mean value ± standard deviation, (*n* = 3). The recovery was calculated on the basis of the obtained results from the Kinetic Spectrophotometric Method.

And confirm the importance of the sensor in terms of cost-effectiveness.

Recovery evaluation for real samples

The method was successfully applied to the determination of TZ in two different commercial food products (powered drink and powdered gelatin samples). To investigate the applicability of the proposed method, recovery experiments were performed using the multiple-point standard addition method. For this purpose, a known amount of TZ was spiked to the formulated preparations, and the total amount of the color was estimated (n=3). The results are summarized in (Table. 4), indicating that the prepared sensor has a very good performance for determining the TZ color in food samples [41,42]. Therefore, the determination of TZ color in samples was confirmed utilizing the standard addition method and then the accuracy of the mentioned method was evaluated by analyzing the samples spiked with the known amount of the TZ. By comparing the results of TZ measurements with the proposed method and evaluating them with T-test, it was found that there is no significant difference, and all t_{exp} values were below t crit (t= 2.77), the result is shown in (Table. 4). So, these results characterized that the applying *Mandarin Leaves*-capped AuNPs sensor

appropriate for the quality control and determination of TZ in color drink and foodstuff samples [12,43].

Comparison of results for this work with other reported sensors

In order to illuminate the applicability and efficiency of biosensor in this work, the results are compared with those of some of the recently reported methods for the reduction of variety of materials by sensor in (Table. 5). Obviously, *Mandarin Leaves*-capped AuNPs shows the shortest time for the reaction in comparison with literature other sensors.

CONCLUSIONS

The investigation in this article focused on measuring the amount of trace tartrazine (TZ) color utilising *Mandarin Leaves*-capped AuNPs sensor, in the company of utilizing sodium borohydride as a stabilizer sensor. A successful analytical method for measuring TZ color was prosperously developed via utilizing a sensitized spectrophotometric with the help of *Mandarin Leaves*-capped AuNPs. The method can be used as an alternative method for (TZ) color measurement owing to advantages like excellent selectivity and sensitivity, low cost, simplicity, low detection limit and no need in utilizing organic harmful solvent or extraction.

Table 5. Comparison of results for this work with other reported sensors.

Samples	Sensor	Time	References
Tartrazine (TZ)	XAD-16 resins	30.0 min	[1]
Tartrazine (TZ)	Active Carbon (AC)	90.0 min	[4]
Malachite green	gold nanoparticles (AuNPs)	15.0 min	[8]
Methyl paraben	*Ricinus Communis*-capeed Fe_3O_4 NPs	12.0 min	[31]
Megestrol drug	*Albizia Lebbeck Leaves*-capped AgNPs	7.0 min	[44]
Methyl paraben and propyl paraben	*Albizia Lebbeck Leaves*-capped AgNPs	60.0 min	[45]
Parabens	*Origanum majorana*-capped AgNPs	65.0 min	[46]
Methyl orange	Seashell -capped AgNPs	11.0 min	[47]
Tartrazine (TZ)	*Mandarin Leaves*-capped AuNPs	7.0 min	Present study

The reaction was evaluated by measuring the absorption rate of tartrazine (TZ) color, the optimum conditions. For determination (TZ) color in the solution we used a prepared from *Mandarin Leaves*-capped AuNPs utilizing sodium borohydride as a stabilizer sensor synthesis and kinetic spectrophotometric method. The standard deviation of (1.9 %), and the detection limit of the method (0.02 µg/L in time 7 min, 385 nm) were obtained for Sensor level response *Mandarin Leaves*-capped AuNPs with (95 %) confidence evaluated. The results of these model surveys show that in modeling by using artificial nerve networks in epoch numbers 10 and 22 experimental points and tension transmission function and the number of 5 neurons in each layer, has the least error rate and the most correlation coefficient equal to 99 percent and the least possible error in simulation with artificial nerve network equal, ANN model as a tool, mean square error (MSE = 0.515) than the other simulated models. The lowest determining error tartrazine (TZ) color could be obtained in a short time, which strongly confirms the greater contribution for the deletion of tartrazine (TZ) color by *Mandarin Leaves*-capped AuNPs sensor. On the other hand, some of the advantages of this work are listed below:

(I) *Mandarin Leaves tree* is very inexpensive, energy saving, and most important of all non-toxic.

(II) Fast and clean synthesis without the use of hazardous, toxic and dangerous compounds or surfactants as a highly stable and reusable eco-friendly catalyst under solvent-free conditions.

(III) *Mandarin Leaves*-capped AuNPs sensor provides several advantages such as simple, mild condition, easy workup, and excellent yield in a short time.

(IV) The use of sodium borohydide extract as an economic and effective reducing and stabilizing agent.

(V) The use of waste *Mandarin Leaves*-capped AuNPs sensor as a natural and inexpensive valuable resource and environmentally benign support.

All these characteristics make *Mandarin Leaves*-capped AuNPs sensor a potential biosensor for tartrazine (TZ) color measurement when juxtaposed against other commercial materials.

Acknowledgments

References

[1] Bişgin A.T., Uçan M., Narin I., Soylak M., A Comparative Study for Separation, Preconcentration and Determination of Tartrazine (E 102) in Soft Drink Samples by Two Kinds of Amberlite Resins, *J. Food Anal. Methods.,* **8:** 2141-2149 (2015).

[2] Banerjee S., Chattopadhyaya M., Adsorption Characteristics for the Removal of a Toxic Dye, Tartrazine from Aqueous Solutions by a Low Cost Agricultural By-Product, *Arab. J. Chem.,* **10:** 1629-1638 (2017).

[3] Nagles E., Ceroni M., Hurtado J., Simultaneous Detection of Tartrazine-Sunset Yellow in Food Samples Using Bioxide/Carbon Paste Microcomposite with Lanthanum and Titanium, *J. Electrochem. Sci. Technol.,* **11(4):** 421-429 (2020).

[4] Chukwuemeka-Okorie H.O., Ekuma F.K., Akpomie K.G., Nnaji J.C., Okereafor A.G., Adsorption of Tartrazine and Sunset Yellow Anionic Dyes onto Activated Carbon Derived fro m Cassava Sievate Biomass, *J. Appl. Water Sci.,* **11:** 3-8 (2021).

[5] Amin K.A., Abdel Hameid H., Abd Elsttar A.H., Effect of Food Azo Dyes Tartrazine and Carmoisine on Biochemical Parameters Related to Renal, Hepatic Function and Oxidative Stress Biomarkers in Young Male Rats, *J. Food Chem. Toxicol.,* **48(10):** 2994-2999 (2010).

[6] Hashemi S.H., Kaykhaii M., Keikha A.J., Parkaz A., Application of Response Surface Methodology to Optimize Pipette Tip Micro Solid Phase Extraction of Dyes from Seawater by Molecularly Imprinted Polymer and their Determination by HPLC, *J. Iran. Chem. Soc.,* **1:** 1-15 (2019).

[7] Heleyel M., Elhami S., Sensitive, Simple and Rapid Colorimetric Detection of Malachite Green in Water Salmon and Canned Tuna Samples based on Gold Nanoparticles, *J. Sci. Food Agric.,* **99(4):** 1919-1925 (2019).

[8] Saleh M.S., Hashem E.Y., Oxidation and Complexation-Based Spectrophotometric Methods for Sensitive Determination of Tartrazine E102 in Some Commercial Food Samples, *Computational Chem.,* **4:** 51-64 (2016).

[9] Hashim K.H., Al-Samrrai Y., Determination of Tartrazine and Sodium Benzoate as Food Additives in some Local Juices using Continuous flow Injection Analysis, *Eng. Agric. Environ. Food.,* **12:** 217–221 (2019).

[10] Dawodu M., Akpomie K., Evaluating the Potential of a Nigerian Soil as an Adsorbent for Tartrazine Dye: Isotherm, Kinetic and Thermodynamic Studies, *Alex. Eng. J.,* **55:** 3211-3218 (2016).

[11] Sahraei R., Farmany A., Mortazavi S.S., A Nanosilver-Based Spectrophotometry Method for Sensitive Determination of Tartrazine in Food Samples, *J. Food Chem.,* **138:** 1239-1242 (2013).

[12] Fooladi E., Ebrahimi M., Nakhaei N., Asadi K., A New Spectrophotometric Method for Determination of Tartrazine in Saffron Samples based on Modified Magnetic Graphene Oxide Nanocomposite, *J. Res. Innova. Food Sci. Technol.,* **9(4):** 389-398 (2021).

[13] Ghoreishi S.M., Behpour M., Golestaneh M., Simultaneous Determination of Sunset Yellow and Tartrazine in Soft Drinks Using Gold Nanoparticles Carbon Paste Electrode, *J. Food Chem.,* **132:** 637-641 (2012).

[14] Altinoz E., Erdemli M.E., Gul M., Erdemli Z., Gul S., Prevention of Toxic Effect of Orally Administered Tartrazine by Crocin in Water Rats, *Toxicol. Environ. Chem.,* **101(3):** 1-19 (2021).

[15] Zeng R., Wang W., Chen M., Tang D., CRISPR-Cas12a-driven MXene-PEDOT: PSS Piezoresistive Wireless Biosensor, *Nano Energy.,* **82:** 105711 (2021).

[16] Shu J., Tang D., Recent Advances in Photoelectrochemical Sensing: from Engineered Photoactive Materials to Sensing Devices and Detection Modes, *Anal. Chem.,* **92(1):** 363-377 (2020).

[17] Yu Zh. Zh., Cai G., Liu X., Tang D., Pressure-Based Biosensor Integrated with a Flexible Pressure Sensor and an Electrochromic Device for Visual Detection, *Anal. Chem.,* **93(5):** 2016-2025 (2021).

[18] Zhang K., Lv Sh., Zhou Q., Tang D., CoOOH Nanosheets-Coated g-C$_3$N$_4$/CuInS$_2$ Nanohybrids for Photoelectrochemical Biosensor of Carcinoembryonic Antigen Coupling Hybridization Chain Reaction with Etching Reaction, *Sens. Actuators. B.,* **307:** 127631 (2020).

[19] Lv Sh., Zhang K., Zhu L., Tang D., ZIF-8-Assisted NaYF4:Yb,Tm@ZnO Converter with Exonuclease III-Powered DNA Walker for Near-Infrared Light Responsive Biosensor, *Anal. Chem.,* **92(1):** 1470-1476 (2020).

[20] Deng H.H., Weng S.H., Huang S.L., Zhang L.N., Liu A.L., Colorimetric Detection of Sulfide based on Target – Induced Shielding Against the Peroxidase – Like Activity of Gold Nanoparticles, *Anal. Chim. Acta.,* **852:** 218-222 (2014).

[21] Arabi M., Ghaedi M., Ostovan A., Development of a Lower Toxic Approach Based on Green Synthesis of Water-Compatible Molecularly Imprinted Nanoparticles for the Extraction of Hydrochlorothiazide from Human Urine, *ACS. Sustainable Chem. Eng.,* **5:** 3775–3785 (2017).

[22] Alkilany A.M., Caravana A.C., Hamaly M.A., Lerner K.T., Thompson L.B., Phase Transfer of Citrate Stabilized Gold Nanoparticles using Nonspecifically Adsorbed Polymers, *J. Colloid. Interface. Sci.,* **46:** 39-44 (2016).

[23] Donga S., Bhadu G.R., Chanda S., Antimicrobial, Antioxidant and Anticancer Activities of Gold Nanoparticles Green Synthesized using Mangifera Indica Seed Aqueous Extract, *Artif. Cells Nanomedici. Biotechnol.,* **48(1):** 1315-1325 (2020).

[24] Farkhari N., Abbasian S., Moshaii A., Nikkhah M., Mechanism of Adsorption of Single And Double Stranded DNA on Gold and Silver Nanoparticles: Investigating Some Important Parameters in Bio – Sensing Applications, *J. Colloids. Surfaces B: Biointerfaces.,* **148:** 657-664 (2016).

[25] Aljabali A.A., Akkam Y., Al Zoubi M.S., Al-Batayneh K.M., Al-Trad B., Abo Alrob O., Alkilany A.M., Benamara M., Evans D.J., Article Synthesis of Gold Nanoparticles using Leaf Extract of Ziziphus zizyphus and Their Antimicrobial Activity, *Nanomaterials.,* **8:** 174 (2018).

[26] Cigeroglu, Z., Ismail K. S., Selin S., Gökben K., Optimization and Kinetic Studies of Ultrasound-Assisted Extraction on Polyphenols from Satsuma Mandarin (Citrus Unshiu Marc.) Leaves, *Iran. J. Chem. Chem. Eng. (IJCCE),* **36(5):** 163-171 (2017).

[27] Xu M., Gao Zh., Zhou Q., Lin Y., Lu M., Tang D., Terbium Ion-Coordinated Carbon Dots for Fluorescent Aptasensing of Adenosine 5'-Triphosphate with Unmodified Gold Nanoparticles, *Biosens. Bioelectron.,* **86:** 978-984 (2016).

[28] Vaibhavkumar N.M., Sanjay J., Suresh K.K., One-Pot Green Synthesis of Carbon Dots by using Saccharum Officinarum Juice for Fluorescent Imaging of Bacteria (Escherichia Coli) and Yeast (Saccharomyces Cerevisiae) Cells, *J. Mater. Sci. Eng.,* **38:** 20-27 (2014).

[29] Mubarak A.D., Thajuddin N., Jeganathan K., Gunasekaran M., Plant Extract Mediated Synthesis of Gold Nanoparticles and its Antibacterial Ctivity Against Clinically Isolated Pathogens, *J. Colloid. Surfaces B: Biointerfaces.,* **85:** 360-365 (2011).

[30] Mombeni Goodajdar B., Marahel F., Niknam L., Pournamdari E., Mousavi E., Ultrasonic Assisted and Neural Network Model for Adsorption of Humic Acid (HAs) by Synthesized CM-β-CD-Fe$_3$O$_4$NPs from Aqueous Solutions, *Int. J. Environ. Anal. Chem.,* **101(11):** 1-17 (2021).

[31] Marahel F., Mombeni Goodajdar B., Basri N., Niknam L., Ghazali A.A., Applying Neural Network Model for Adsorption Methyl Paraben (MP) Dye using *Ricinus Communis*-Capeed Fe$_3$O$_4$NPs Synthesized from Aqueous Solution, *Iran. J. Chem. Chem. Eng. (IJCCE),* **41(7):** 2358-2377 (2022).

[32] Marahel F., Mombeni Goodajdar B., Niknam L., Faridnia M., Pournamdari E., Mohammad Doost S., Ultrasonic Assisted Adsorption of Methylene Blue Dye and Neural Network Model for Adsorption of Methylene Blue Dye by Synthesized Mn-Doped PbS nanoparticles, *Int. J. Environ. Anal. Chem.,* **103(13):** 3059-3080 (2023).

[33] Khodadadi B., Sabeti M., Norozi O., Biosynthesis of Ag Nanoparticles at Ziziphus Jujuba Kernel Substrate using Tilia platyphyllos Extract: Catalytic Activity for Reduction of Organic Dyes, *J. Appl. Chem. Res.,* **15(1):** 46-63 (2021).

[34] Khodadadi B., Bordbar M., Nasrollahzadeh M., Achillea millefolium L., Extract Mediated Green Synthesis of Waste Peach Kernel Shell Supported Silver Nanoparticles: Application of the Nanoparticles for Catalytic Reduction of a Variety of Dyes in Water, *J. Colloid. Interface. Sci.,* **493:** 85-92 (2017).

[35] Mishra A., Tripathy S.K., Yun S.I., Bio-Synthesis of Gold and Silver Nanoparticles from Candida Guilliermondii and their Antimicrobial Effect Against Pathogenic Bacteria, *J. Nanosci. Nanotechnol.,* **11(1):** 243–248 (2011).

[36] Patra J.K., Baek K.H., Novel Green Synthesis of Gold Nanoparticles using Citrullus Lanatus Rind and Investigation of Proteasome Inhibitory Activity, Antibacterial, and Antioxidant Potential, *Int. J. Nanomedicine.,* **10:** 7253–7264 (2015).

[37] Shahrouei F., Elhami S., Tahanpesar E., Highly Sensitive Detection of Ceftriaxone in Water, Food, Pharmaceutical and Biological Samles Based on Gold Nanoparticles in Aqueous and Micellar Media, *J. Spectrochim. Acta. A. Mol. Biomolecules. Spectrosc.,* **203:** 287-293 (2018).

[38] Fouladgar M.D., Nanostructured Sensor for Simultaneous Determination of Trace Amounts of Bisphenol A and Vitamin B6 in Food Samples, *J. Food Anal. Methods.,* **10:** 1507–1514 (2017).

[39] Mehedi N., Mokrane N., Alami O., Ainad-Tabet S., Zaoui C., Kheroua O., Saidi D., A Thirteen Week Ad Libitum Administration Toxicity Study of Tartrazine in Swiss Mice, *Africa. J. Biotechnol.,* **12:** 4519-4529 (2013).

[40] Leulescu M., Morıntale E., Rotaru A., Palarie I., Moant A., Florian G., Cioatera N., Harabor A., Popescu M., Rotaru P., Tartrazine: Physical, Thermal and Biophysical Properties of the Most Widely Employed Synthetic Yellow Food-Colouring Azo Dye, *J. Therm. Anal. Calorimetr.,* **134:** 209-231 (2018).

[41] Ghonimi W.A.M., Elbaz A., Histological Changes of Selected Westar Rat Tissues Following the Ingestion of Tartrazine with Special Emphasis on the Protective Effect of Royal Jelly and Cod Liveroil, *J. Cytol. Histol.,* **6(4):** 346-349 (2015).

[42] Li J.S., Lau Y.Q., Sun T.Y., Chen C.S., Purification and Biochemical Characterization of an Alkaline Feruloyl Esterase from Penicillium Sumatrense NCH-S₂ Using Rice Bran as Substrate, *CyTA – J. Food.,* **19(1):** 1-10 (2021).

[43] Qiu Z., Shu J., He Y., Lin Z., Zhang K., Lv Sh., Tang D., CdTe/CdSe Quantum Dot-Based Fuorescent Aptasensor with Hemin/G-Quadruplex DNzyme for Sensitive Detection of Lysozyme Using Rolling Circle Amplification and Strand Hybridization, *Biosensors and Bioelectronics.,* **87:** 18-24 (2017).

[44] Niknam L., Marahel F., Applying Kinetic Spectrophotometric Method for Megestrol Drug with *Albizia Lebbeck Leaves*-capped AgNPs Sensor Synthesis in Urine and Blood Samples, *J. Phys. Theor. Chem.*, **18(1):** 37-50 (2021).

[45] Maghami F., Abrishamkar M., Mombeni Goodajdar B., Hossieni M., Simultaneous Adsorption of Methylparaben and Propylparaben Dyes from Aqueous Solution using Synthesized *Albizia lebbeck* Leaves-Capped Silver Nanoparticles, *Desal. Water Treat.,* **223:** 388-392 (2021).

[46] Karachi N., Motahari S., Nazarian S., Working for the Betterment of Simultaneous Deletion of Paraben Dyes from Industrial Effluents on to *Origanum majorana*-Capped Silver Nanoparticles, *Desal Water Treat.,* **228:** 389-402 (2021).

[47] Rostami-Vartooni A., Nasrollahzadeh M., Alizadeh M., Green Synthesis of Seashell Supported Silver Nanoparticles using Bunium Persicum Seeds Extract: Application of the Particles for Catalytic Reduction of Organic Dyes, *J. Colloid Interface Sci.*, **470:** 268-275 (2016).